JOURNAL OF VIROLOGY, Apr. 2006, p. 4174–4178 Vol. 80, No. 8
0022-538X/06/$08.00+0 doi:10.1128/JVI.80.8.4174–4178.2006

Role of Endosomal Cathepsins in Entry Mediated by the Ebola Virus Glycoprotein

Kathryn Schornberg,[1] Shutoku Matsuyama,[2] Kirsten Kabsch,[2] Sue Delos,[2] Amy Bouton,[1]*† and Judith White[1,2]*†

Departments of Microbiology[1] and Cell Biology,[2] University of Virginia, Charlottesville, Virginia 22908-0734

Received 17 December 2005/Accepted 29 January 2006

Using chemical inhibitors and small interfering RNA (siRNA), we have confirmed roles for cathepsin B (CatB) and cathepsin L (CatL) in Ebola virus glycoprotein (GP)-mediated infection. Treatment of Ebola virus GP pseudovirions with CatB and CatL converts GP1 from a 130-kDa to a 19-kDa species. Virus with 19-kDa GP1 displays significantly enhanced infection and is largely resistant to the effects of the CatB inhibitor and siRNA, but it still requires a low-pH-dependent endosomal/lysosomal function. These and other results support a model in which CatB and CatL prime GP by generating a 19-kDa intermediate that can be acted upon by an as yet unidentified endosomal/lysosomal enzyme to trigger fusion.

The Ebola virus glycoprotein (GP) is a class I viral fusion protein composed of a receptor binding subunit (GP1) and a fusion subunit (GP2) that are linked by a disulfide bond. There are three well-characterized means by which class I viral fusion proteins are triggered for fusion: exposure to low pH, interaction with receptors at neutral pH, and a two-step process that involves interaction with receptors at neutral pH followed by exposure to low pH, as reviewed in reference 3. Previous work has shown that low endosomal pH is required for infection mediated by vesicular stomatitis virus (VSV) pseudovirions bearing Ebola virus GP (VSV-GP), but it is not sufficient to trigger GP-mediated cell-cell fusion (17). Moreover, low pH does not induce fusion of red blood cells to GP-expressing cells, even if the cells are engineered to express the influenza hemagglutinin precursor to provide strong red cell binding. Low pH also does not overcome a bafilomycin block to infection of prebound VSV-GP, performed in either a one-step (21) or a two-step (10, 13) paradigm (data not shown). These observations, together with the finding that elimination of the furin cleavage site between GP1 and GP2 does not ablate infection (14, 22), led us to suspect that low pH is required for optimal functioning of endosomal proteases. A survey of class-specific protease inhibitors revealed that agents that target endosomal cysteine proteases (leupeptin, E64d, and MG132) inhibited infection by VSV-GP, while agents that target serine or aspartyl proteases or the proteasome did not (data not shown). This suggested that endosomal cysteine proteases might be required for Ebola virus GP-mediated infection. Indeed, while our work was in progress, Chandran et al. showed that two endosomal cysteine proteases, cathepsin B (CatB) and cathepsin L (CatL), are required for infection mediated by Ebola virus GP (2). CatB and CatL are ubiquitously expressed across the wide range of cells susceptible to Ebola virus infection (12), and they have previously been shown to be involved in the entry of reovirus (4). CatL has also recently been shown to be involved in entry mediated by the severe acute respiratory syndrome (SARS) coronavirus spike glycoprotein (16) as well as in processing the fusion glycoprotein of Hendra virus (15).

Using VSV pseudotypes bearing full-length Ebola virus GP or VSV G and encoding GFP (VSV-GP and VSV-G, respectively), we first confirmed a need for CatB and CatL in infection mediated by Ebola virus GP. As seen in Fig. 1A, infection by VSV-GP was greatly reduced in the presence of the CatB inhibitor CA074Me and was also reduced, although to a lesser extent, in the presence of the CatL inhibitor Z-FY(*t*-Bu)-dmk. Infection by VSV-G was not affected by either of these inhibitors at the same concentrations. We next used small interfering RNA (siRNA) duplexes to more specifically knock down the expression of CatB and/or CatL in Vero cells. CatB protein levels were reduced between 50 to 90% in CatB siRNA-treated cells with an average of 83% reduction in CatB activity (Fig. 1B, lane 2). In the presence of CatB siRNA, CatL protein levels and activity were consistently elevated (lane 6). CatL expression was reduced between 70 to 100% in cells treated with CatL siRNA, coincident with a 98% reduction in CatL activity (lane 7). CatB expression and activity were largely unaffected by CatL siRNA (lane 3). In cells treated with combined CatB and CatL siRNAs, both CatB and CatL expression and activity were reduced by at least 90% (lanes 4 and 8). Infection by VSV-GP was reduced by an average of 80% in CatB siRNA-treated cells and 46% in CatL siRNA-treated cells (Fig. 1C). When cells were treated with a combination of CatB and CatL siRNA, infection by VSV-GP was reduced by an average of 89%. Infection by VSV-G was not significantly reduced with any of these treatments. These siRNA data confirm roles for CatB and CatL in Ebola virus GP-mediated infection of primate (Vero) cells and are in agreement with Chandran et al., who found similar requirements using mouse embryo fibroblasts from CatB and CatB/CatL knockout mice (2).

CatB and CatL could be required to activate cellular proteins involved in viral entry and/or to process Ebola virus GP as a prelude to fusion. Therefore, we first tested whether CatB

* Corresponding author. Mailing address: University of Virginia, 1300 Jefferson Park Ave., Charlottesville, VA 22908-0734. Phone: (434) 924-2593. Fax: (434) 982-3912. E-mail for A. Bouton: ahb8y@virginia.edu; E-mail for J. White: jw7g@virginia.edu.
† Equal contributors.

and CatL could digest Ebola virus GP in vitro. Treatment of purified VSV-GP with CatB alone digested GP1 from a 130-kDa species to a 50-kDa species with some digestion to a 19-kDa species (Fig. 2A, lane 3). Treatment with CatL alone digested GP1 predominantly to a 20-kDa species (lane 4). Combined digestion with CatB plus CatL produced a strong doublet comprised of the 19-kDa and 20-kDa forms (lane 5). Digestion of VSV-GP with CatB plus CatL appeared to be processive, as seen by the time-dependent appearance of the 20-kDa form followed by the 19-kDa form (Fig. 2B, lanes 3 to 6). Longer film exposures show that accumulation of the 20-kDa and 19-kDa forms was accompanied by the progressive loss of the 130-kDa and then the 50-kDa forms of GP1 (data not shown). We hypothesize that the 50-kDa species represents removal of the O-linked glycosylation-rich mucin-like domain of GP1, as genetic deletion of this region results in a GP1 species of similar size (8). Interestingly, treatment of VSV-GP with the bacterial enzyme thermolysin, which has low cleavage specificity, also generated a 19-kDa form of GP1 (Fig. 2B, lane 2). This suggests that there may be a specific region of GP1 that is hypersensitive to protease digestion, as has been seen for reovirus (4–7). Treatment of VSV-GP with CatB plus CatL for extended periods of time resulted in a significant reduction of GP1 after 60 min and a loss of detectable GP1 after 120 min (Fig. 2C, lanes 8 and 9). Importantly, the fusion subunit GP2 was significantly reduced in virus samples treated with CatB plus CatL for 120 min where GP1 was completely proteolyzed (lane 9).

To test whether in vitro cleavage of GP circumvented the requirement for CatB and/or CatL during the process of viral entry, VSV-GP was either mock treated (no enzyme) or treated with CatB plus CatL or thermolysin for 20 min (conditions generally yielding maximal, although not complete, conversion to the 19-kDa form of GP1) prior to infection of cells treated with CatB and CatL inhibitors or siRNAs. Treatment of VSV-GP with CatB plus CatL or thermolysin led to a dramatic and reproducible enhancement of infection, on average a 20-fold increase over mock-treated virus (Fig. 3A and data not shown; note that for these experiments the MOI was 10-fold lower than that used in Fig. 1). Since VSV-GP bearing 19-kDa GP1 is still highly infectious, we postulate that the 19-kDa GP1 fragment contains the 150 amino acids from the amino-terminal end of GP1 that is predicted by Manicassamy and coworkers to contain the receptor binding domain (9). The enhancement of infection could be at least partly due to the removal of the mucin-like domain of GP1, as we and others have observed that virus particles pseudotyped with a form of Ebola virus GP that lacks the mucin-like domain have increased titers over virus particles bearing wild-type Ebola virus GP (2, 8). Importantly, infection with CatB plus CatL- or thermolysin-treated virus was significantly enhanced, even in the presence of the CatB inhibitor (Fig. 3A) and CatB siRNA (data not shown) but was only slightly enhanced in the presence of CatL inhibitor or siRNA compared to mock-treated virus. When the percent of infected inhibitor- or siRNA-treated cells was normalized to the percent of infected control-treated cells, the difference in resistance of CatB plus CatL- or thermolysin-treated virus (i.e., with 19-kDa GP1) to the CatB inhibitors compared to the CatL inhibitors was more evident (Fig. 3B and C). Acquisition of resistance to the CatB inhibitor and siRNA correlated with conversion to the 19-kDa form, and not the 20-kDa form, of GP1 (data not shown). Importantly, infection by pseudovirions bearing 19-kDa GP1 was still inhibited by bafilomycin and the general cysteine protease inhibitor

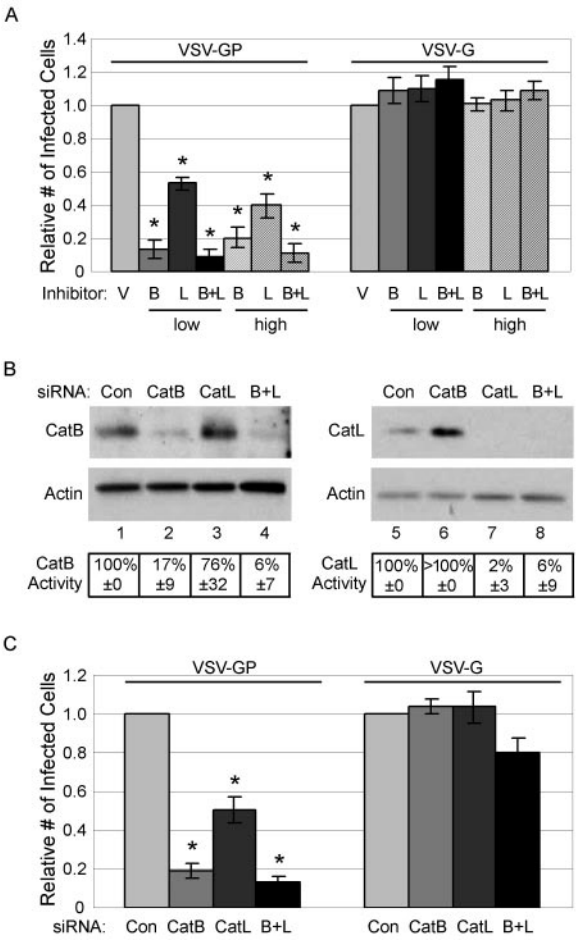

FIG. 1. Effect of cathepsin inhibitors and siRNA on infection of Vero cells by VSV-GP. (A) Cells were pretreated for 2 h at 37°C with vehicle alone (V), CatB inhibitor (B), or CatL inhibitor (L) at low concentrations (0.5 μM CatB inhibitor, 1 μM CatL inhibitor) and high concentrations (1 μM CatB inhibitor, 4 μM CatL inhibitor). Cells were washed and infected with VSV-GP and VSV-G pseudovirions at approximate multiplicities of infection (MOI) of 0.2 to 0.4 and 0.5 to 1.0, respectively, in the presence of fresh inhibitors. Twenty-four hours postinfection, the cells were fixed and the percentage of GFP-positive cells was determined by flow cytometry. Results shown are the averages of normalized data from three to six experiments, where the average percent infection for vehicle-treated cells was 31 ± 19 for VSV-GP and 56 ± 10 for VSV-G. Error bars indicate standard errors, and asterisks indicate a statistically significant deviation from the mean relative to vehicle-treated cells at a confidence level of greater than 99%. (B and C) Cells were transfected with a nontargeting control siRNA oligonucleotide (Con) or siRNA oligonucleotides targeting CatB and/or CatL. Seventy-two hours posttransfection, the cells were either lysed for Western blotting and activity assays (B) or infected as described for panel A (C). (B) Representative blot of CatB and CatL expression in siRNA-treated cells and the average results from five activity assays ± the standard deviation. Results shown in panel C are the averages of normalized data from three to six experiments, where the average percent infection for control siRNA-treated cells was 23 ± 14 for VSV-GP and 53 ± 6 for VSV-G. Error bars indicate the standard errors, and asterisks indicate a statistically significant deviation from the mean relative to control siRNA-treated cells at a confidence level greater than 99%.

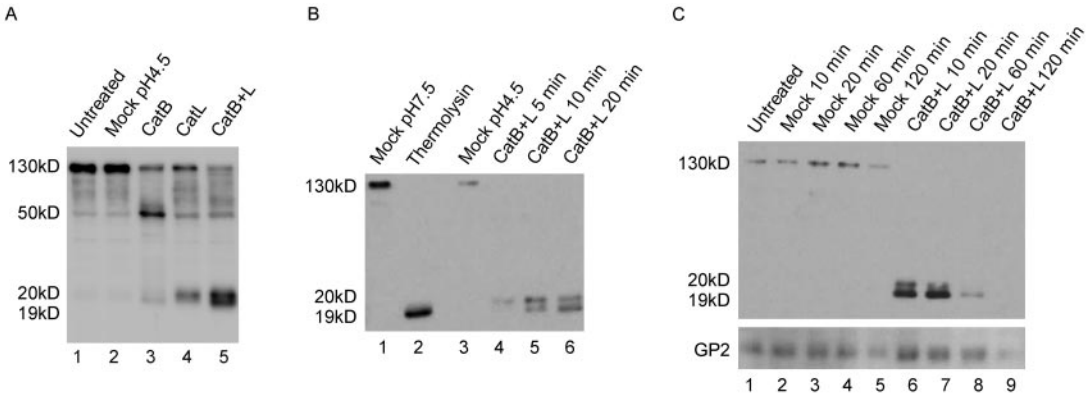

FIG. 2. Cleavage of Ebola virus GP by CatB and CatL. (A) VSV-GP was treated with no enzyme (mock) or 20 μg/ml CatB, CatL, or CatB plus CatL (CatB+L) at pH 4.5 with 4 mM dithiothreitol for 10 min at 37°C. Reactions were quenched, and samples were analyzed by Western blotting for GP1. (B) VSV-GP was treated with 20 μg/ml CatB plus CatL in the above conditions for 5, 10, or 20 min or with 0.5 mg/ml thermolysin at pH 7.5 for 20 min. Mock treatments were performed in the same buffers containing no enzyme. Reactions were quenched and analyzed by Western blotting for GP1. (C) VSV-GP was mock treated or treated with 25 μg/ml CatB plus CatL as described above for 10, 20, 60, or 120 min. Reactions were quenched and analyzed by Western blotting for GP1 and GP2. The variable staining intensities of the 130-kDa versus the 19-kDa forms of GP1 could be due to the polyclonal GP1 antibody reacting more strongly with the 19-kDa form or to differing efficiencies of transfer between the high- and low-molecular-mass forms.

E64d (Fig. 3D). This suggests that, while CatB and CatL digest GP to a highly active 19-kDa form that is largely independent of CatB, there is still a need for a cellular factor(s) whose function (e.g., zymogen activation) requires low pH and an E64d-inhibited activity.

Based on these data, we favor a two-step model in which cleavage of GP1 by CatB plus CatL primes GP by generating a key 19-kDa GP1 intermediate, while a third endosomal/lysosomal factor triggers fusion (Fig. 4A). This differs significantly from the model proposed by Chandran et al. (2), in which cleavage by CatL (or CatB) generates an 18-kDa GP1 intermediate and in which further cleavage by CatB triggers fusion (Fig. 4B). This group found that, after formation of an 18-kDa intermediate, continued proteolysis by CatB digested GP1 to a form that was no longer detectable by Western blotting and inactivated the virus. They suggested that inactivation of infectivity was due to premature deployment of the fusion machinery. In the model proposed by Chandran et al., CatB and CatL are therefore both necessary and sufficient for infection. However, we have been able to trap a 19-kDa GP1 species (Fig. 4A) that promotes enhanced infectivity that is largely independent of the requirement for further action by CatB. This suggests that some factor other than CatB is required to trigger fusion. One possible explanation for the difference between our work and that of Chandran et al. is that the 18-kDa species generated by Chandran et al. (Fig. 4B, royal blue) may be equivalent to our 20-kDa intermediate (Fig. 4A, royal blue). The difference in apparent molecular mass could be due to the removal of an N-linked oligosaccharide chain in their 18-kDa species caused by treatment with N-glycosidase F. While in our hands digestion with CatB plus CatL resulted in the capture of a highly active 19-kDa species that is largely independent of further need for CatB (Fig. 4A), Chandran et al. did not detect a subsequent discrete digestion product beyond their 18-kDa species. This difference could be due to our use of high-specific-activity CatB or to other technical differences. Importantly, because extensive digestion with CatB plus CatL removes all detectable GP1 from the viral particle (Fig. 2C in this study, Fig. 2E from the Chandran et al. study), it is formally possible that the lack of infectivity observed by Chandran et al. under these conditions may have arisen from an inability of the virus to bind to target cells. Moreover, under conditions where we were able to show loss of detectable GP1 (prolonged digestion of the virus with CatB and CatL; see Fig. 2C), we also observed significant loss of GP2. If the proteolysis performed by Chandran et al. resulted in a similar loss of GP2, the virus would therefore likely be unable to complete the fusion step even if it could bind. Based on these factors, we favor the model presented in Fig. 4A, in which CatB and CatL are necessary, but not sufficient, for infection and in which an additional factor is required to trigger fusion.

The model proposed in Fig. 4A postulates that there is an additional, as yet unknown, cellular factor that triggers primed GP for fusion. A potential candidate for this second step is a lysosomal thiol reductase, akin to what has recently been shown with the Env glycoprotein of murine leukemia virus (18, 19). In the case of murine leukemia virus, receptor binding to the SU subunit primes Env for subsequent triggering by isomerization of the SU-TM disulfide bond by an internal thiol reductase activity. We propose that, for Ebola virus GP, CatB and CatL cleavage of the GP1 subunit primes GP by exposing a critical disulfide bond (perhaps the disulfide bond that links GP1 and GP2), making it accessible to reduction by a lysosomal thiol reductase, such as gamma-interferon-inducible lysosomal thiol reductase (1). Reduction would then relieve the GP1 clamp, thus allowing conformational changes in the GP2 subunit that trigger fusion (Fig. 4A). Our data with thermolysin-treated virus indicate that other proteases are also able to "prime" GP1, as has been shown for reovirus (4–7) and severe acute respiratory syndrome virus (11). This could potentially result in a lack of efficacy of inhibitors of viral entry that are targeted solely to CatB and/or CatL. Work is currently under way to identify the protein(s) involved in the trigger step and to evaluate this step as a potential target for fusion inhibitors.

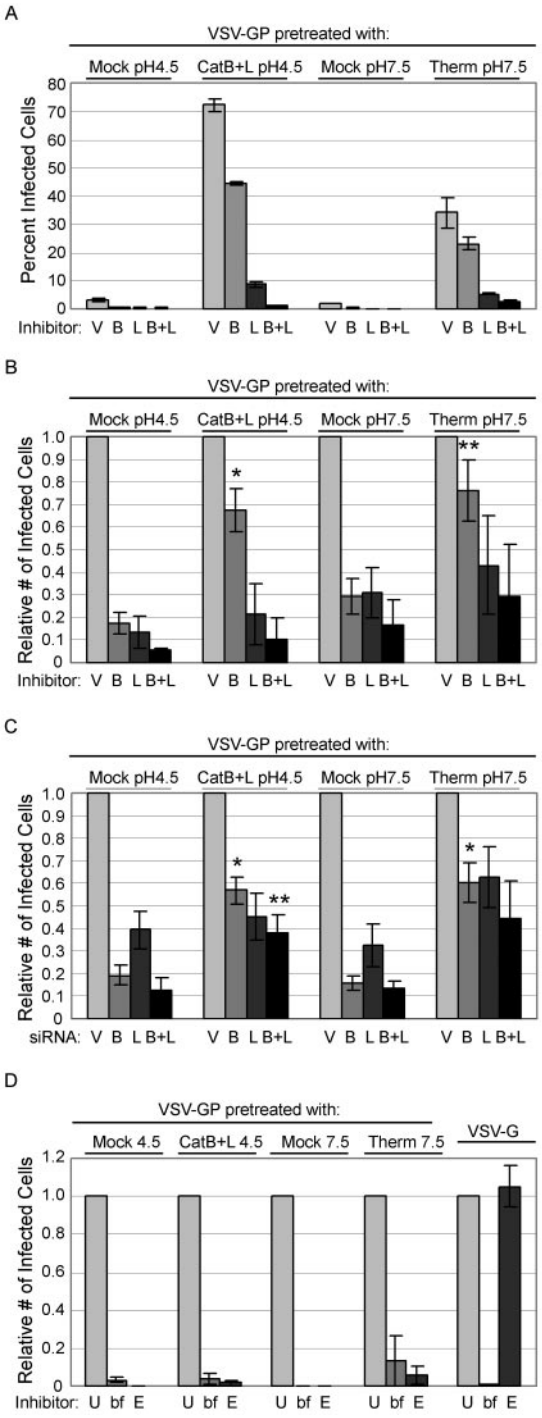

FIG. 3. Effects of inhibitors and siRNA on infection by protease-treated VSV-GP. VSV-GP was treated with no enzyme, 20 μg/ml CatB plus CatL (CatB+L), or 0.5 mg/ml thermolysin (Therm) for 20 min as described in the text. (A) Vero cells were treated with vehicle alone (V) or CatB (B) and CatL (L) inhibitors as described in the legend to Fig. 1A (1 μM CatB inhibitor and 4 μM CatL inhibitor) and then infected with mock-treated or protease-treated VSV-GP at an MOI of 0.02 to 0.04 (note that this is a 10-fold lower MOI than that used for experiments in Fig. 1 to enable quantification of enhanced infection). Twenty-four hours postinfection, the percentage of GFP-positive cells was determined by flow cytometry. Data shown are the averages of duplicate infections from one representative experiment. Error bars indicate the standard error. (B and C) Vero cells were treated with CatB (B) and CatL (L) inhibitors (B) or siRNA (C) as described in the legend to Fig. 1 and infected with protease-treated VSV-GP as described for panel A. Results shown are the averages of normalized data from three to five experiments; panel B includes the data presented in panel A. Error bars indicate the standard errors, and asterisks indicate a statistically significant deviation from the mean of respective mock-treated virus infections at a confidence level greater than 98% (*) or 94% (**). We note that stronger inhibition by the CatL chemical inhibitor is seen in panel B than that seen in Fig. 1B. This may be due to the lower MOI used in this experiment. (D) Vero cells were left untreated (U) or were pretreated for 2 h at 37°C with 200 nM bafilomycin (bf) or 50 μM E64d (E) and then infected with protease-treated VSV-GP as described above or with VSV-G at an MOI of 0.5 to 1. Twenty-four hours postinfection, the percentage of GFP-positive cells was determined by fluorescence microscopy. Results shown are the averages of normalized data from two to three experiments, and error bars indicate standard errors.

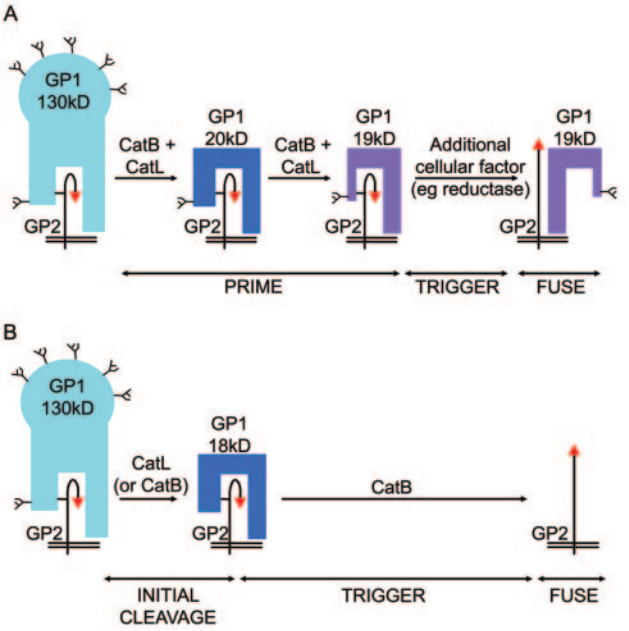

FIG. 4. Models of GP-mediated fusion. (A) In our model, initial cleavage of GP1 (by CatB, CatL, or other proteases) removes the mucin-like domain generating a 50-kDa species (not shown). This 50-kDa species is then primed by CatB plus CatL (or another protease) cleavage of GP1 to produce 20-kDa (royal blue) and then 19-kDa (purple) forms of the glycoprotein. This primed form of GP is then acted upon by an additional cellular factor, such as a lysosomal thiol reductase, which reduces a critical disulfide bond, possibly the disulfide bond between GP1 and GP2. This reduction relieves the GP1 clamp, thus allowing conformational changes in GP2 that expose and reposition the fusion peptide (red arrowhead) and trigger fusion. (B) In the model proposed by Chandran et al. (2), initial cleavages by CatB and/or CatL generate an 18-kDa GP1 intermediate (royal blue, which we hypothesize is equivalent to our 20-kDa intermediate with one N-linked glycosylation site removed). Further cleavage by CatB completely digests GP1, thereby removing the clamp and allowing fusion. N-linked glycosylation sites in GP1 are depicted with short branched black lines.

Reagents. Control nontargeting small interfering RNA (siRNA) oligonucleotides, SMARTpool oligonucleotides consisting of four different siRNA oligonucleotides targeting CatB, and an siRNA oligonucleotide targeted to nucleotides

98 to 116 of the human cathepsin L cDNA sequence (15) were purchased from Dharmacon. Antibodies to CatB and CatL were purchased from Athens Research and Technology. The polyclonal GP1 antibody, raised against sGP-Fc, was a gift from Paul Bates, University of Pennsylvania. The rabbit polyclonal GP2 antibody was raised against the six-helix bundle core of the GP2 subunit (cDNA encoding the six-helix bundle construct was a gift from Peter Kim, Massachusetts Institute of Technology). Innozyme CatB and CatL activity assay kits (Calbiochem) were used to measure CatB and CatL enzyme activities according to the manufacturer's directions.

VSV pseudotypes and infections. VSV pseudotypes encoding green fluorescent protein (GFP) and complemented with the glycoproteins of Ebola virus Zaire (VSV-GP) or VSV (VSV-G) were made in BHK-21 cells as described previously (17). The virus-containing supernatants were harvested and concentrated by pelleting through a 20% sucrose cushion. Virus stocks were titered by infecting Vero cells with serial dilutions and counting GFP-positive cells by flow cytometry or fluorescence microscopy (typical titers for VSV-GP were 10^8 IU/ml and were 10^9 IU/ml for VSV-G) and stored in aliquots at −80°C in 10% sucrose. VSV-GP and VSV-G were used to infect Vero cells at approximate multiplicities of infection (MOIs) of 0.2 to 0.4 and 0.5 to 1.0, respectively, in Dulbecco's modified Eagle medium plus 5% fetal bovine serum, unless otherwise indicated. Twenty-four hours postinfection, the cells were fixed and the percentage of GFP-positive cells was determined by counting 5,000 to 10,000 cells per sample by flow cytometry.

Cell treatments. For chemical inhibitor experiments, Vero cells were pretreated with vehicle alone (dimethyl sulfoxide), the CatB inhibitor CA074Me (Calbiochem), and/or the CatL inhibitor Z-FY(*t*-Bu)-dmk (Calbiochem) at the indicated concentrations for 2 h at 37°C. Cells were infected with VSV-GP and VSV-G in the presence of fresh inhibitors, as described above. For siRNA experiments, Vero cells were transfected with a nontargeting control siRNA oligonucleotide or siRNA oligonucleotides targeting CatB and/or CatL at 100 nM final concentrations using Transit TKO (Mirus Corporation). Seventy-two hours posttransfection, the cells were infected with VSV-GP and VSV-G as described above.

In vitro proteolysis of GP. VSV-GP was treated with 20 μg/ml CatB (specific activity, 914 U per mg) and CatL (specific activity, 3.8 U per mg) (Athens Research and Technology), unless otherwise indicated, at pH 4.5 in HEPES-MES buffer (40 mM HEPES, 40 mM morpholinepropanesulfonic acid [MES], 50 mM NaCl) with 4 mM dithiothreitol or with 0.5 mg/ml thermolysin (Sigma) in HEPES-MES buffer at pH 7.5 for the indicated times at 37°C. The reactions were neutralized by the addition of 2 M Tris, pH 8.0, and 50 μM E64 or with the addition of 0.5 mM EDTA, respectively. Mock treatments were conducted in the same buffers but contained no enzyme. Virus samples were then analyzed by Western blotting as described previously (20) or were used to infect Vero cells at an approximate MOI of 0.02 to 0.04 (based on the titer of untreated virus) as described above.

We thank Robert Netter and Paul Bates for the GP1 antibody, Peter Kim for the GP2 six-helix bundle construct used to make the immunogen for the GP2 antiserum, Gary Nabel for the plasmid encoding Ebola virus Zaire GP, and Michael Whitt for the VSV pseudotyping system and associated protocols. We thank Zaoying Chen for several preparations of VSV-GP pseudotypes and Cara Pager and Rebecca Dutch for sharing the CatL siRNA sequence prior to publication.

Work was supported by grants from the NIH to J.M.W. (AI055925 and AI22470) and A.H.B. (AI050733). K.S. and K.K. were supported in part by training grants for infectious diseases (5T32 AI07046) and biodefense (5T32 AI055432), respectively. S.M. was supported by a fellowship from the Japan Society for the Promotion of Science.

REFERENCES

1. **Arunachalam, B., U. T. Phan, H. J. Geuze, and P. Cresswell.** 2000. Enzymatic reduction of disulfide bonds in lysosomes: characterization of a gamma-interferon-inducible lysosomal thiol reductase (GILT). Proc. Natl. Acad. Sci. USA **97:**745–750.
2. **Chandran, K., N. J. Sullivan, U. Felbor, S. P. Whelan, and J. M. Cunningham.** 2005. Endosomal proteolysis of the Ebola virus glycoprotein is necessary for infection. Science **308:**1643–1645.
3. **Earp, L. J., S. E. Delos, H. E. Park, and J. M. White.** 2005. The many mechanisms of viral membrane fusion proteins. Curr. Top. Microbiol. Immunol. **285:**25–66.
4. **Ebert, D. H., J. Deussing, C. Peters, and T. S. Dermody.** 2002. Cathepsin L and cathepsin B mediate reovirus disassembly in murine fibroblast cells. J. Biol. Chem. **277:**24609–24617.
5. **Golden, J., and L. Schiff.** 2005. Neutrophil elastase, an acid-independent serine protease, facilitates reovirus uncoating and infection in U937 promonocyte cells. Virol. J. **2:**48. http://www.virologyj.com/content/2/1/48.
6. **Golden, J. W., J. A. Bahe, W. T. Lucas, M. L. Nibert, and L. A. Schiff.** 2004. Cathepsin S supports acid-independent infection by some reoviruses. J. Biol. Chem. **279:**8547–8557.
7. **Jane-Valbuena, J., L. A. Breun, L. A. Schiff, and M. L. Nibert.** 2002. Sites and determinants of early cleavages in the proteolytic processing pathway of reovirus surface protein σ3. J. Virol. **76:**5184–5197.
8. **Jeffers, S. A., D. A. Sanders, and A. Sanchez.** 2002. Covalent modifications of the Ebola virus glycoprotein. J. Virol. **76:**12463–12472.
9. **Manicassamy, B., J. Wang, H. Jiang, and L. Rong.** 2005. Comprehensive analysis of Ebola virus GP1 in viral entry. J. Virol. **79:**4793–4805.
10. **Matsuyama, S., S. E. Delos, and J. M. White.** 2004. Sequential roles of receptor binding and low pH in forming prehairpin and hairpin conformations of a retroviral envelope glycoprotein. J. Virol. **78:**8201–8209.
11. **Matsuyama, S., M. Ujike, S. Morikawa, M. Tashiro, and F. Taguchi.** 2005. Protease-mediated enhancement of severe acute respiratory syndrome coronavirus infection. Proc. Natl. Acad. Sci. USA **102:**12543–12547.
12. **McGrath, M. E.** 1999. The lysosomal cysteine proteases. Annu. Rev. Biophys. Biomol. Struct. **28:**181–204.
13. **Mothes, W., A. L. Boerger, S. Narayan, J. M. Cunningham, and J. A. Young.** 2000. Retroviral entry mediated by receptor priming and low pH triggering of an envelope glycoprotein. Cell **103:**679–689.
14. **Neumann, G., H. Feldmann, S. Watanabe, I. Lukashevich, and Y. Kawaoka.** 2002. Reverse genetics demonstrates that proteolytic processing of the Ebola virus glycoprotein is not essential for replication in cell culture. J. Virol. **76:**406–410.
15. **Pager, C. T., and R. E. Dutch.** 2005. Cathepsin L is involved in proteolytic processing of the Hendra virus fusion protein. J. Virol. **79:**12714–12720.
16. **Simmons, G., D. N. Gosalia, A. J. Rennekamp, J. D. Reeves, S. L. Diamond, and P. Bates.** 2005. Inhibitors of cathepsin L prevent severe acute respiratory syndrome coronavirus entry. Proc. Natl. Acad. Sci. USA **102:**11876–11881.
17. **Takada, A., C. Robison, H. Goto, A. Sanchez, K. G. Murti, M. A. Whitt, and Y. Kawaoka.** 1997. A system for functional analysis of Ebola virus glycoprotein. Proc. Natl. Acad. Sci. USA **94:**14764–14769.
18. **Wallin, M., and E. M. H. Garoff.** 2004. Isomerization of the intersubunit disulphide-bond in Env controls retrovirus fusion. EMBO J. **23:**54–65.
19. **Wallin, M., R. Loving, M. Ekstrom, K. Li, and H. Garoff.** 2005. Kinetic analyses of the surface-transmembrane disulfide bond isomerization-controlled fusion activation pathway in Moloney murine leukemia virus. J. Virol. **79:**13856–13864.
20. **Weidow, C. L., D. S. Black, J. B. Bliska, and A. H. Bouton.** 2000. CAS/Crk signalling mediates uptake of Yersinia into human epithelial cells. Cell Microbiol. **2:**549–560.
21. **White, J., J. Kartenbeck, and A. Helenius.** 1980. Fusion of Semliki forest virus with the plasma membrane can be induced by low pH. J. Cell Biol. **87:**264–272.
22. **Wool-Lewis, R. J., and P. Bates.** 1999. Endoproteolytic processing of the Ebola virus envelope glycoprotein: cleavage is not required for function. J. Virol. **73:**1419–1426.